Int. J. Electrochem. Sci., 13 **(2018)** 11193 – 11202, doi: 10.20964/2018.11.73

International Journal of
ELECTROCHEMICAL
SCIENCE
www.electrochemsci.org

Fabrication of a Highly Sensitive Electrochemical Immunosensor for Human Epididymis Protein 4 (HE4) Detection

Jian Qu and Feng Yu[*]

Department of Gynecology, Affiliated Hospital of Jining Medical University, 89 Guhuai Road, Jining, Shandong, 272100, P.R. China
[*]E-mail: yfengguhuaijin@163.com

Received: 29 November 2017 / *Accepted:* 3 January 2018 / *Published:* 1 October 2018

Diagnostics of ovarian cancer can be achieved by detecting the level of human epididymis protein 4 (HE4). The present study proposed the preparation of a biosensor based on a nitrogen-doped graphene/gold nanoparticle (AuNP)/fluorine-doped tin oxide (FTO) glass electrode modified with fructosyl amino-acid oxidase (FAO), i.e., the AuNPs/N-doped GNs/FTO. The proposed electrode was found to be highly sensitive and selective towards the biosensing of HE4, with a the limit of detection (LOD) calculated at 1.21 μg/mL and a linear detection range of 10 to 65 μg/mL.

Keywords: Human epididymis protein 4; Fructosyl amino-acid oxidase; Electrochemical sensor; Nanocomposite; Nitrogen-doped graphene

1. INTRODUCTION

Ovarian cancer (OC), the sixth most common gynaecological malignancy, is characterized by an incidence rate that increases with age and post-menopausal status. In brief, the crude incidence rate varies over a range of 4.7 per 100 000 (in women <50 years of age) and 29.6 per 100 000 (in the age group of 50–64 years) [1, 2]. Among the gynaecological malignancies that have caused death, OC has ranked in first place; considering the asymptomatic property at early stages, along with the absence of effective screening methods, approximately 75% of the patients are diagnosed at an advanced stage [3, 4]. Additionally, the net discrepancy between survival rates in early and advanced stages was found to be 80–90% *vs.* 15–20%, respectively, necessitating the construction of screening programmes and/or the discrimination between malignancy and benign pelvic masses by developing highly accurate biomarkers [5, 6]. Recently, various biomarkers have been reported for the diagnosis of women with

suspected OC [7, 8], among which human epididymis protein 4 (HE4) has gained the most attention. Initially, the detection of HE4 was aimed at improving the diagnostic specificity of CA-125 for a comparable sensitivity [9-12]. Due to its homology with some secreted serine protease inhibitors, it shows a lower expression in normal ovarian tissue, ovarian benign disease and low-malignant potential tumours, whilst amplified expression in some CA-125-deficient OCs [13, 14]. Preliminary investigations have been carried out on the immunohistochemical and genomic properties of HE4 [15, 16], and substantial research has been based on these findings. In addition, HE4 has been suggested as an aid in OC diagnosis according to recently published guidelines on a meta-analytical method [17].

For the detection of HE4, many different strategies have been reported, such as ion-exchange and boronated affinity chromatography, electrophoresis and fluorescence [6, 8, 18-20]. Unfortunately, the above strategies suffer many disadvantages, including high cost, requirement of blood specimen pretreatment, professional manipulation, and prolonged detection time. Therefore, it is necessary to develop a highly selective and sensitive disposable in vitro biosensor for the HE4 analysis. Additionally, other favourable properties are also needed, such as rapid analysis (within seconds) and a small specimen volume (e.g., 10–15 μL of blood or other physiological fluid).

The preparation of electrochemical biosensors towards the detection of HE4 has been reported; the preparation is based on the surface modification via a bio-recognition mechanism using sugar-binding materials (mostly boronic acid), proteins and antibodies that are specific to HE4. A transduction mechanism is then typically introduced, such as amperometry/voltammetry, impedometry, or potentiometry[21, 22]. Recently, a new generation of biosensors under the mechanism of direct electron transfer between the electrode and biomolecule, necessitates the development of biocompatible nanomaterials. Among them, graphene nanosheets (GNs), a 2D nanomaterial, has been developed for many different fields, including biosensors, chemical and physics (classical electronics and bio electronics) processes, as a remarkable biocompatible nanomaterial [23-25]. An accurate modification can be performed by doping a carbon-based material, resulting in an effective change of its intrinsic properties, for instance, the modification of the structural framework of the material's surface and its electronic properties. The GNs interlayers would be converted into GN-based hybrid materials after the introduction of metal nanoparticles, thereby avoiding aggregation [26-28]. The direct and uniform attachment of gold nanoparticles (AuNPs) onto the high density GNs can be achieved, considering the strong binding between the GNs and metal nanoparticles; therefore, an excellent immobilization scaffold can be constructed for the protein.

In the present report, the N-doped GNs with AuNPs, through an ethylene glycol reduction process, was reported, along with its application in the detection of HE4. Characterizations were performed using different methods, including a spectrophotometer, UV–vis, and X-ray diffraction (XRD). Following the immobilization of the enzyme, cyclic voltammetry (CV) and electrochemical impedance spectroscopy (EIS) measurements were carried out. The results confirmed the effective electrochemical response of the developed AuNPs/GNs composite film towards the biosensing of the target HE4 in human blood specimens.

2. EXPERIMENTS

2.1. Reagents

Urea, chitosan, 4-aminoantipyrine, proteases, graphite, ethylene glycol (EG), $HAuCl_4$, MES (4-morpholinoethane sulfonic acid), Dess-Martin periodinane, pyridine, and L-valine were commercially available from Sigma Chemical Co. Human epididymis protein 4 (HE4), bovine serum albumin (BSA), fructosyl-amino acid oxidase (FAO), glutaraldehyde (GA) and fluorine-doped tin oxide (FTO) glass electrodes were commercially available from Sigma-Aldrich. An HE4 ELISA kit was purchased from Shanghai Kanu Biotech Co., Ltd. Distilled water (DW) was used throughout the preparation of the test solutions.

2.2. Preparation of the N-doped graphene nanosheets (GNs)

For the preparation of graphene, concentrated sulfuric acid (50 mL) was added to 2.0 g graphite in a 250 mL conical flask, which was then vigorously agitated at 25 °C. Subsequently, this flask was further poured carefully and slowly into a solution with 2.0 g $NaNO_2$ and 6.0 g $KMnO_4$ under gentle mixing, with the yielded mixture subject to a heating treatment for 20 h at 25 °C. This was followed by a dropwise addition of DW (80 mL) into the solution, maintained for 15 min. Following the addition of H_2O_2 (20 mL, 30%), the reaction mixture was washed once using a hydrochloric acid solution and three times using DW. The resulting precipitate was suspended in DW via an ultra-sonication route, and used to prepare an aqueous graphene dispersion (5 mg/mL). A one pot method was employed for the synthesis of the high N content graphene, with a chemical dopant of urea [29]. The GN dispersion was mixed with GNs (10 mL, 50 mg) dispersed in 25 mL of DW and urea (2 g), and sonicated for 240 min. The obtained mixture was potted in a 50 mL Teflon-lined autoclave, and maintained for 300 min at 150 °C. The solids (N-doped GNs) were filtered, followed by washing using DW (three times). The resulting product (N-doped GNs) was left drying at 55 °C in a vacuum oven.

2.3. Synthesis of N-doped GNs embedded with AuNPs (AuNPs/N-doped GNs)

The collective addition of the gold-precursor salts and GNs in the EG solution aimed to provide convincing evidence for the functionalization of AuNPs on the N-doped GNs [30]. Briefly, the N-doped GNs (50 mg) were infused into an aqueous $HAuCl_4$ solution (50 mL, 0.02 mM) and the obtained mixed solution was subjected to ultrasonication for 120 min until a steady colloid was generated. This was followed by injecting the EG (20 mL) into the mixed solution, with continuous mixing for another 120 min. The obtained produced was kept for 360 min at 130 °C and continuously stirred. After filtration, the resulting AuNPs/N-doped GNs composites were formed, and washed with DW.

2.4. Enzyme immobilization

The FTO electrode was completely cleaned with acetone in an ultrasonic bath for 10 min, along with DW for another 10 min. This was followed by the electrochemical deposition of the as-prepared AuNPs/N-doped GNs on three test electrodes submerged in an electrochemical cell via chronoamperometry, at an applied potential of −0.6 V (against the Ag/AgCl reference electrode). The working and counter electrodes were an FTO electrode (area, 1 cm^2) and a Pt wire, respectively. A freshly coated film was used after drying at ambient temperature. The optimization of the enzyme concentration was carried out using different concentrations of enzyme (5, 15, 25, and 35 IU).

For the preparation of a 1% chitosan solution (*w*/*v*), chitosan was dissolved in 1% (v/v) acetic acid under ultrasonication for 60 min and vortexed. The FTO electrode, drop-casted with chitosan solution (4 μL) was then dried at 30 °C for 12 h. During the preparation of biosensors, BSA (4%) and FAO (1%) were used to prepare an enzyme solution containing BSA (25U FAO/100 μL enzyme solution). A GA solution (2.5%) was then added into the as-prepared enzyme solution (GA to FAO solution ratio, 1:2) for 30 min (30 °C). This was followed by spreading 2 μL of the as-prepared mixture onto the FTO electrode, which was then dried at 4 °C for 240 min. The resulting electrode was denoted as AuNPs/N-doped GNs/FTO**.**

2.5. Analysis

The crystal property of the nanocomposite was measured by an X-ray diffractometer (D8 – Advance XRD, Bruker, Germany) with a Cu Kα radiation, whilst the optical features were studied using a UV-Vis spectrophotometer (Halo RB-10). Electrochemical experiments were carried out using a CH Instruments 660A electrochemical Workstation (CHI-660 A) equipped with a three-electrode assembly, where the reference and auxiliary electrodes were an Ag/AgCl (3 M KCl) electrode and a platinum wire, respectively. To study the charge transfer on the surface of the bare and modified electrode, EIS was carried out at an amplitude of 5 mV and a frequency range of 10^1 to 10^5 Hz (supporting electrolyte, 0.1 M KCl; probe, 5 mM $[Fe(CN)_6]^{3-/4-}$). DPV measurements were also carried out with a potential range from -0.6 to 0.4 V, where the step potential and pulse amplitude were 2 mV and 50 mV, respectively. We also applied a 50 ms pulse, a scan rate of 10 mV/s, and a sampling time of 10 ms, along with a 100 ms pulse interval. For the optimization process, the DPV measurements were carried out at different electrolyte pH values, incubation times and incubation temperatures.

3. RESULTS AND DISCUSSION

As shown in the XRD pattern, a typical sharp peak of 2 theta at 13.4 degrees was observed, corresponding to the presence of graphene oxide. However, as shown in Figure 1A, this peak was found to shift to the right and convert into a broad peak after further heating and doping with nitrogen, which suggested that the graphene oxide (GO) was reduced into graphene. The arrangement of relative peak intensities and peak positions of GNs was consistent with that of the standard JCPDS, and no

impurities were observed. The diffraction peaks from numerous planes and d-values accurately matched JCPDS reported data for GNs [31]. As shown in the UV–vis spectrum, a peak was observed at 228 nm, ascribed to the π–π* transition of GO and an absorption peak was observed at 307 nm, suggesting the n-π* transition of the C–O bonds, and the embedding through exfoliation and inclusion on the graphene. The peak at 275 nm suggested that the GO was reduced into the graphene after the doping of N. An additional 535 nm peak resulted from the AuNPs, as shown in Figure 1B.

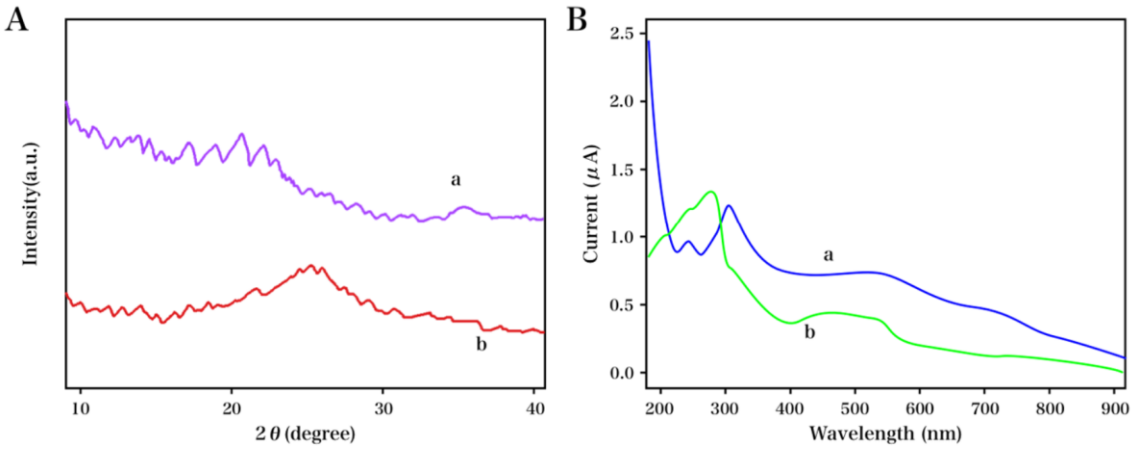

Figure 1. (A) XRD pattern recorded for the graphene oxide and N-doped GNs. (B) Absorption spectra recorded for the graphene oxide and AuNPs/N-doped GNs in aqueous solution.

EIS has been accepted as a conventional method to the investigate the stepwise modification process, where the electrode interface features would change. Experiments were carried out in a 0.1 M KCl solution with 5 mM $Fe(CN)_6^{4-/3-}$ as the redox probe, and a frequency range between 0.1 Hz and 10^5 Hz was used, with a signal amplitude of 5 mV. As shown in Figure 2, the diameter of the semicircle, calculated from the Nyquist plot, corresponds to the electron transfer resistance (R_{ct}) [23]. For the bare FTO electrode, the electron transfer resistance (R_{ct}) was obtained as 1007 Ω. For the N-doped GNs and AuNPs/N-doped GNs/FTO electrodes, the R_{ct} was reduced to 221 Ω and 114 Ω, respectively (Figure 3), which suggested that the charge transfer between the electrode surface and the electrolyte, in the case of the nanocomposites, was relatively faster. The obtained results were consistent with this theory, confirming the positive effect of the as-prepared AuNPs/GNs composite on the improvement of interfacial electron transfer [25]. For the AuNPs/N-doped GNs/FTO, the R_{ct} was increased to 448 Ω, which suggested that a barrier layer of FAO molecules was formed, blocking the access of the charge transfer.

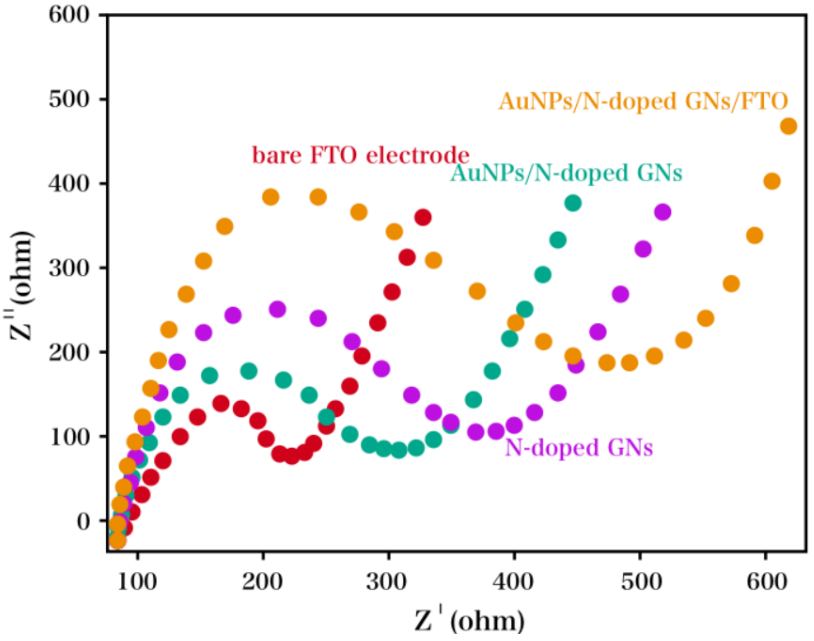

Figure 2. EIS Nyquist plots recorded for the bare FTO electrode, N-doped GNs, AuNPs/N-doped GNs and AuNPs/N-doped GNs/FTO in 0.1 M KCl containing 5 mM $[Fe(CN)_6]^{3/4}$, using 5 mV amplitude of sine voltage signal at a frequency range of 0.1 Hz to 100 kHz.

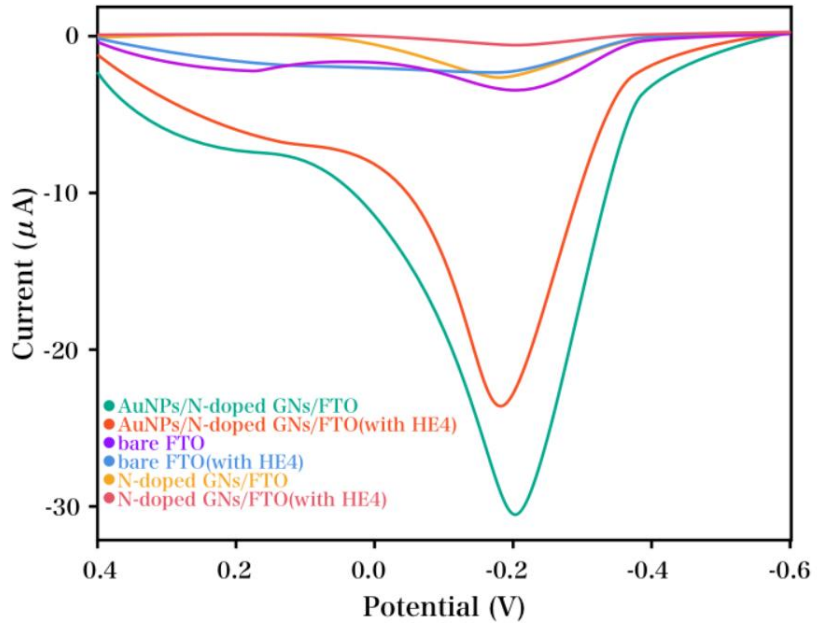

Figure 3. DPV recorded for AuNPs/N-doped GNs/FTO, bare FTO and N-doped GNs/FTO in 0.1 M pH 8.0 phosphate buffer in the presence and absence of the HE4 solution (50 μg/mL).

DPV profiles were plotted for the AuNPs/N-doped GNs/FTO in the absence and presence of HE4 in 0.1 M pH 8.0 phosphate buffer, as shown in Figure 3. After adding the target HE4, the oxidation peak current of the developed electrode was sharply reduced, suggesting that access of the

charge transfer was impeded by the protein molecules. This result also confirmed the binding of HE4 onto the surface of the electrode, thus the proposed electrochemical method can be applied to the analysis of HE4. For comparison, for the bare FTO and AuNPs/N-doped GNs/FTO, only low current responses were observed before or after the addition of HE4. These could be attributed to the low loading of HE4 on the bare FTO and N-doped GNs/FTO electrodes, demonstrating that the N-doped GNs played a key role for electro-catalytic determination.

The pH effect on the current response of our developed biosensor was studied by measuring its influence on the binding of HE4 to the test electrode. The percentage of decreased current $I_d=(I_0-I_a)/I_0$ was utilized as the binding parameter, where I_d was the fractional decrease in current, I_0 was the current in the absence of HE4, and I_a was the current in the presence of HE4. As shown in Figure 4A, the pH effect on the current response was studied over a pH range of 5 to 9. With increasing pH, a gradual increase in the value of I_d was observed, which is in accordance with the findings that the binding of boronic acid with the diol of HbA_{1c} occurred under weak alkaline conditions [32]. However, with further pH increase, the value of I_d was reduced. Therefore, the optimum pH value was obtained as 8, considering the maximal current response. We also investigated the incubation time effect on the current response. As indicated in Figure 4B, an increase in the value of I_d was recorded with time, reaching a plateau after 0.5 h. Therefore, the incubation time was optimized as 0.5 h and used in further measurements. We continued to study the incubation temperature effect on the current response of the test electrode. As shown in Figure 4C, as the temperature increased over a range of 5 to 30 °C, a slight increase in the value of I_d was observed. Further temperature rise led to the reduction of I_d due to the thermal deactivation of HE4. Thus, the incubation temperature was optimized at 30 °C.

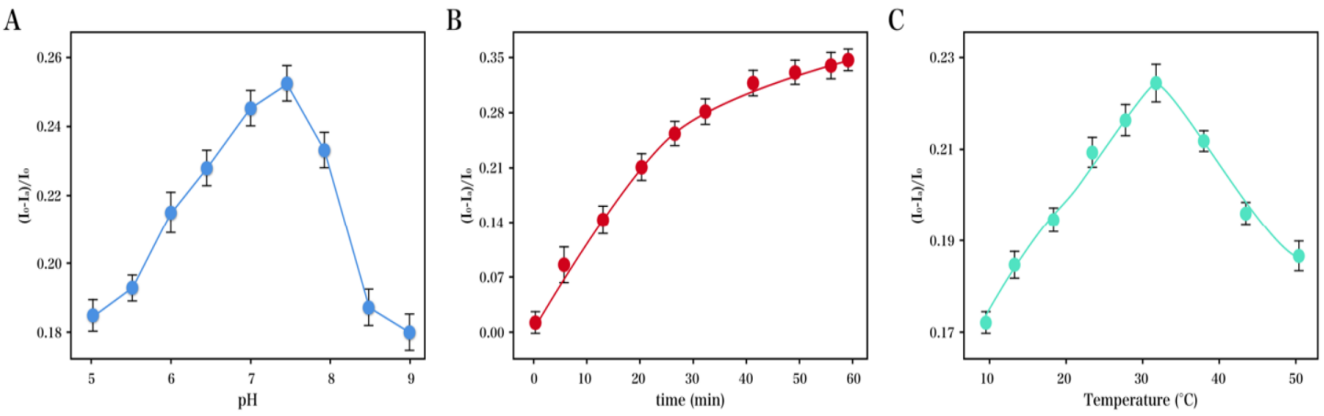

Figure 4. Effects of (A) pH value in 0.1 M phosphate buffer; (B) reaction time in 0.1 M pH 8.0 phosphate buffer; (C) reaction temperature in 0.1 M pH 8.0 phosphate buffer on the performance of the developed electrode toward the analysis of HE4.

DPV was recorded for the performance of our proposed electrode towards the detection of varying concentrations of the target HE4 under the optimum parameters. As the concentration of the HE4 increased, a decrease in the oxidation peak current was observed (Figure 5A). As shown in Figure 5B, a linear relationship was found between the concentration of HE4 and the value of I_d over a range of 10 to 65 μg/mL. At higher concentrations, a curvature was recorded, since the active sites on the

electrode surface for target binding decreased. Based on a S/N of 3, the limit of detection (LOD) was calculated as 1.70 μg/mL. These results suggested a similar sensitivity to those reported elsewhere as shown in Table 1 (Supporting information). In terms of human blood specimens, the physiological levels of HE4 are found in a range of 3 to 13 mg/mL. Therefore, the developed strategy could be used for the detection of the HE4 in real blood specimens after dilution with the buffer solution.

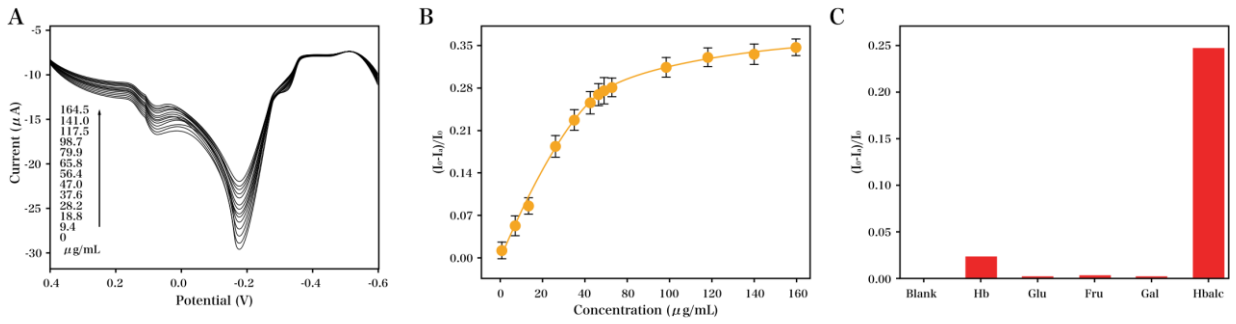

Figure 5. (A) DPV curves recorded for HE4 with an increasing concentration in phosphate buffer (0.1 M, pH 8.0) using the developed electrode. (B) Linear calibration plot of I_d against HE4 concentration. (D) Selectivity of the developed electrode towards HE4 in the presence of glucose, Hb, galactose and fructose in phosphate buffer (0.1 M, pH 8.0).

The selectivity of our proposed method towards the detection of HE4 was studied using several interferents under comparable parameters. A comparative analysis was made on the electrochemical response of HE4 in the presence of glucose, Hb, galactose and fructose (Figure 5C). The detection of HE4 was not affected by the three smaller interferents, shown by a minimal electrochemical response of their binding onto the electrode surface. On the other hand, Hb led to a slight I_d increase, however, this small increase can be neglected. These results confirmed the acceptable selectivity of our proposed electrode, and its potential for further detection of HE4 in real biological specimens.

Table 1. Performance comparison of different electrode toward the analysis of target HE4.

Method	Linear range	Detection limit	Reference
Localized surface plasmon resonance biosensor	10 pM to10,000 pM	100 pM	[33]
Enzyme-linked immunosorbent assay	0.3-10 μM	141.5 pM	[34]
Enzyme linked immunosorbent assay	0.1-1.0 μg/mL	—	[35]
Sandwich enzyme-linked immunosorbent assay	5-10μg/mL	—	[19]
AuNPs/N-doped GNs/FTO	10-65 μg/mL	1.21μg/mL	This work

We further studied the repeatability, reproducibility and long-term stability of the developed sensor through the measurement of the current response to HE4 (50 μg/mL) in 0.1 M pH 8.0 phosphate buffer. After nine consecutive experiments, the relative standard deviation (RSD) was obtained as 3.1% (Table 2), showing an acceptable repeatability. To study the sensor reproducibility, six different modified electrodes were used for parallel tests, with a corresponding RSD of 6.6% (Table 3). After storage at 4 °C for 1 month, the proposed electrode was found to retain *ca.* 98% of the initial voltammetric response, suggesting a desirable long-term stability of the developed electrode. For comparison purposes, a HE4 ELISA kit was used for determining HE4 (50 μg/mL). The result showed that the proposed electrochemical method has similar performance when compared to the commercial HE4 ELISA kit.

Table 2. AuNPs/N-doped GNs/FTO for nine consecutive determination of 50 μg/mL HE4 (n=3).

Number	RSD (%)	Number	RSD (%)	Number	RSD (%)
1	2.7	4	1.7	7	2.6
2	1.5	5	1.6	8	2.4
3	0.9	6	3.1	9	0.9

Table 3. Six AuNPs/N-doped GNs/FTO for 50 μg/mL HE4 determination (n=3).

Number	RSD (%)	Number	RSD (%)	Number	RSD (%)
1	5.4	3	2.4	5	1.6
2	6.6	4	4.7	6	3.1

4. CONCLUSIONS

The present study reported a sensitive AuNPs/N-doped GNs/FTO interface for the electrochemical analysis of HE4. The FAO was immobilized through a cross-linking strategy, making the working electrode more stable. Our developed biosensor was found to be highly selective and sensitive towards the analysis of the HE4 target. In addition, this voltammetric biosensor has the advantages of low cost and simplicity, considering the accessible detection chemicals and simple filtration process.

References

1. S. Ferraro, F. Braga, M. Lanzoni, P. Boracchi, E.M. Biganzoli and M. Panteghini, *Journal of Clinical Pathology*, 66 (2013) 273.
2. J. Lin, J. Qin and V. Sangvatanakul, *European Journal of Obstetrics Gynecology & Reproductive Biology*, 167 (2013) 81.
3. S. Zhen, L. Bian, L. Chang and X. Gao, *Molecular & Clinical Oncology*, 2 (2014) 559.
4. H. Zhuang, Z. Hu, M. Tan, L. Zhu, J. Liu, D. Liu, L. Yan and B. Lin, *Biochimie*, 105 (2014) 91.
5. A.C. Macedo, R.M. Da, S. Lumertz and L.R. Medeiros, *International Journal of Gynecological Cancer Official Journal of the International Gynecological Cancer Society*, 24 (2014) 1222.
6. K.D. Steffensen, M. Waldstrøm, I. Brandslund, B. Lund, S.M. Sørensen, M. Petzold and A.

Jakobsen, *Oncology Letters*, 11 (2016) 3967.
7. L.T. Jia, Y.C. Zhang, J. Li, Y. Tian and J.F. Li, *Clinical & Translational Oncology*, 18 (2016) 233.
8. C. Yong, Q. Chen, Q. Liu and G. Feng, *Tumor Biology*, 37 (2016) 8359.
9. Q. Fan, G. Luo, T. Yi, Q. Wang, D. Wang, G. Zhang, X. Jiang and X. Guo, *Biomedical Reports*, 7 (2017) 67.
10. P. Innao, M. Pothisuwan and P. Pengsa, *Asian Pacific Journal of Cancer Prevention Apjcp*, 17 (2016) 4483.
11. A. Shahi, N. Bahrami, A. Fakharian, S. Sharifynia, E. Moslemi, A. Izadi, A. Khosravi, H. Jamaati and A. Mohamadnia, *Open Journal of Clinical Diagnostics*, 07 (2017) 83.
12. Z. Yang, C. Wei, Z. Luo and L. Li, *Oncotargets & Therapy*, 6 (2013) 957.
13. S. Michienzi, R. Falzarano, V. Viggiani, D. Rossini, F. Longo and E. Anastasi, *Biochimica Clinica*, 37 (2013) 195.
14. A. Stiekema, C.A. Lok, G.G. Kenter, W.J. van Driel, A.D. Vincent and C.M. Korse, *Gynecologic Oncology*, 132 (2014) 573.
15. P.L. Li, X. Zhang, T.F. Li, L.L. Wang, L.T. Du, Y.M. Yang, J. Li, H.Y. Wang, Y. Zhang and C.X. Wang, *Clinica Chimica Acta*, 439 (2015) 148.
16. K. Beata, F. Malgorzata, S. Piotr, S. Beata, J.G. Joanna, S. Maciej and K. Maria, *European Journal of Obstetrics Gynecology & Reproductive Biology*, 194 (2015) 141.
17. A.E. Leon, E. Squarcina, T. Maggino, C. Romagnolo, L.D. Pup, S. Cervo, M. Gion and A.S.C. Fabricio, *Biochimica Clinica*, 37 (2013) 200.
18. Y. Tian, C. Wang, L. Cheng, A. Zhang, W. Liu, L. Guo, H. Ye, Y. Huang, J. Chen and X. Wen, *Journal of Ovarian Research*, 8 (2015) 72.
19. L.Z. †, Z.L. †, S. Jing, X. Ying, X. Luo, Y. Zhang, H. Yang, W. Zhang, S. Luo and J. Fang, *Journal of Clinical Laboratory Analysis*, 30 (2015) 581.
20. S.I. Choi, M.A. Jang, B.R. Jeon, H.B. Shin, Y.K. Lee and Y.W. Lee, *Annals of Laboratory Medicine*, 37 (2017) 526.
21. L. Lu, B. Liu, J. Leng, K. Wang, X. Ma and S. Wu, *Microchim. Acta.*, 183 (2016) 837.
22. R. Drapkin, H.H. von Horsten, Y. Lin, S.C. Mok, C.P. Crum, W.R. Welch and J.L. Hecht, *Cancer Research*, 65 (2005) 2162.
23. Y. Zhang, G.M. Zeng, L. Tang, J. Chen, Y. Zhu, X.X. He and Y. He, *Anal. Chem.*, 87 (2015) 989.
24. H. Bai, C. Wang, J. Chen, J. Peng and Q. Cao, *Biosensors & Bioelectronics*, 64 (2015) 352.
25. M.B. Gholivand, N. Karimian and M. Torkashvand, *Journal of Analytical Chemistry*, 70 (2015) 384.
26. X. Li, X. Wang, L. Li, H. Duan and C. Luo, *Talanta*, 131 (2015) 354.
27. Z. Zhang, R. Cai, F. Long and J. Wang, *Talanta*, 134 (2015) 435.
28. S. Qi, B. Zhao, H. Tang and X. Jiang, *Electrochimica Acta*, 161 (2015) 395.
29. L. Sun, L. Wang, C. Tian, T. Tan, Y. Xie, K. Shi, M. Li and H. Fu, *Rsc Advances*, 2 (2012) 4498.
30. Y. Li, W. Gao, L. Ci, C. Wang and P.M. Ajayan, *Carbon*, 48 (2010) 1124.
31. P. Kannan, T. Maiyalagan, N.G. Sahoo and M. Opallo, *Journal of Materials Chemistry B*, 1 (2013) 4655.
32. S. Liu, U. Wollenberger, M. Katterle and F.W. Scheller, *Sensors and Actuators B: Chemical*, 113 (2006) 623.
33. J. Yuan, R. Duan, H. Yang, X. Luo and M. Xi, *International Journal of Nanomedicine*, 7 (2012) 2921.
34. X. Liu, F. Zhao, L. Hu and Y. Sun, *Oncotargets & Therapy*, 8 (2015) 1239.
35. J. Bai, *Chinese Journal of Obstetrics & Gynecology & Pediatrics*, 4 (2015) 514.